

Optical trapping, Field enhancement and Laser cooling in photonic crystals

Ovidiu Toader and Sajeev John

*Department of Physics, University of Toronto, 60 St. George Str.,
Toronto, M5S 1A7 Canada*

ovi@physics.utoronto.ca, john@physics.utoronto.ca

Kurt Busch

*Institut für Theorie der Kondensierten Materie, Universität
Karlsruhe, P.O. Box 6980, 76128 Karlsruhe, Germany*

kurt@tkm.physik.uni-karlsruhe.de

Abstract: We present a detailed study of the mode structure of inverse opal photonic crystal materials with an emphasis on their potential use in optical trapping and cooling. In particular, we analyze the modes corresponding to the upper and lower band edges of a high refractive index inverse opal, i.e., the so-called “air” and “dielectric” bands. In the dielectric band, we demonstrate optical intensity enhancements of two orders of magnitude which may facilitate nonlinear optical effects in the solid. In the air band, dipolar optical trapping potentials for cold atoms in the voids arise when these modes are excited by an external laser field. In addition, we discuss aspects of atom cooling through the polarization gradients provided by these modes. The results suggest that optical trapping and cooling may be achieved within a photonic crystal using a single laser source.

© 2001 Optical Society of America

OCIS codes: (260.2110) Electromagnetic theory, (020.7010) Trapping, (140.7010) Trapping, (140.3320) Laser cooling

References and links

1. S. John, “Strong localization of photons in certain disordered dielectric superlattices,” *Phys. Rev. Lett.* **58**, 2486–2489 (1987).
2. E. Yablonovitch, “Inhibited spontaneous emission in solid-state physics and electronics,” *Phys. Rev. Lett.* **58**, 2059–2062 (1987).
3. S. John and T. Quang “Collective Switching and Inversion without Fluctuation of Two-Level Atoms in Confined Photonic Systems,” *Phys. Rev. Lett.* **78**, 1888–1891 (1997).
4. S. Chu, “The manipulation of neutral particles,” *Rev. Mod. Phys.* **70**, 685–706 (1998).
5. C.N. Cohen-Tannoudji, “Manipulating atoms with photons,” *Rev. Mod. Phys.* **70**, 707–720 (1998).
6. W.D. Phillips, “Laser cooling and trapping of neutral atoms,” *Rev. Mod. Phys.* **70**, 721–742 (1998).
7. K. Busch and S. John, “Photonic band gap formation in certain self-organizing systems,” *Phys. Rev. E* **58**, 3896–3908 (1998).
8. J.D. Joannopoulos, P.R. Villeneuve, and S. Fan, “Photonic Crystals: Putting a new twist on light,” *Nature* **386**, 143 (1997).
9. K. M. Ho, C. T. Chan, and C. M. Soukoulis, “Existence of a photonic gap in periodic dielectric structures,” *Phys. Rev. Lett.* **65**, 3152–3155 (1990).
10. R. D. Meade, A. M. Rappe, K.D. Brommer, and J. D. Joannopoulos, “Accurate theoretical analysis of photonic band-gap materials,” *Phys. Rev. B* **48**, 8434–8437 (1993).
11. Harold J. Metcalf and Peter van der Straten, *Laser Cooling and Trapping* (Springer-Verlag, New York, 1999).

Photonic crystals are a novel class of optical materials with two or three-dimensional periodic dielectric modulation. As a consequence, the dispersion relation and the corresponding spatial electromagnetic mode structure of photonic crystals exhibit substantial deviations from those of ordinary vacuum or homogeneous dielectric material. The electromagnetic properties may be engineered through a choice of dielectric materials, lattice type and topology leading to the possibility of light localization [1]. Such an engineering of the spectral and spatial properties of the electromagnetic field also affects the coupling between radiation and matter [2]. For instance, a suitably designed photonic crystal may exhibit a complete photonic band gap (PBG), i.e., a range of frequencies for which linear propagation in any direction is forbidden. If the transition frequency of an excited atom embedded in such a photonic crystal lies within the complete PBG, spontaneous emission may be completely suppressed [2] and a bound photon-atom state is formed instead. Based on these principles, numerous applications such as the design of zero-threshold microlasers, light emitting diodes that exhibit coherence properties on the single photon level, sub-picosecond all-optical switches, and all-optical transistors have been suggested[3].

While the above applications rely on strong modifications of the photonic density of states, very little attention has been paid to possible applications of the detailed electromagnetic mode structure of photonic crystals. Over the past years, the technology of optical trapping and cooling of atoms through the engineering of intensity and/or polarization gradients in the electromagnetic mode structure has witnessed tremendous progress [4, 5, 6] such as the guiding and interference of coherent matter waves and Bose-Einstein condensation of neutral atoms.

In this paper we analyze the potential of photonic crystal to allow control over the motion of atoms located inside such a crystal. For concreteness, we choose to study the inverse opal photonic crystal whose spectral properties have recently been studied in great detail [7]. However, the main concepts are of direct relevance to other photonic crystals. In section **1** we introduce the theoretical description of photonic crystal which we apply in section **2** to visualize the optical intensity of the electric field for the modes at the lower and upper band edge of an inverse opal, respectively. In section **3**, we analyze the polarization properties of the modes mentioned above. We isolate and visualize a region in the crystal that exhibits polarization gradients suitable for laser cooling.

1 Theoretical description of photonic crystals

The electromagnetic properties of the photonic crystals are completely determined by the solutions of the macroscopic Maxwell's equations [8]. We consider the case of a photonic crystal made from non-magnetic materials that are characterized by frequency independent dielectric constants. The periodicity of the dielectric function is described by the Bravais lattice associated with the crystal. In the absence of external sources, the equation for the magnetic field may be written as:

$$\vec{\nabla} \times \left(\frac{1}{\epsilon(\vec{r})} \vec{\nabla} \times \vec{H}_\omega(\vec{r}) \right) = \left(\frac{\omega}{c} \right)^2 \vec{H}_\omega(\vec{r}) . \quad (1)$$

Here, $\vec{H}_\omega(\vec{r})$ is the magnetic field of the mode with frequency ω and $\epsilon(\vec{r})$ is the spatially periodic dielectric function that describes the crystal. In addition, $\vec{H}_\omega(\vec{r})$ satisfies the transversality condition $\vec{\nabla} \cdot \vec{H}_\omega(\vec{r}) \equiv 0$. The periodicity of the dielectric function requires the solution of Eq. (1) to satisfy the Bloch-Floquet theorem:

$$\vec{H}_\omega(\vec{r}) = e^{i\vec{k} \cdot \vec{r}} \vec{H}_{\omega, \vec{k}}(\vec{r}) , \quad (2)$$

where, \vec{k} is the Bloch vector (crystal momentum) and is restricted to lie in the first Brillouin zone (BZ). $\vec{H}_{\omega, \vec{k}}$ denotes the lattice periodic part of the Bloch function, i.e., $\vec{H}_{\omega, \vec{k}}(\vec{r} + \vec{R}) = \vec{H}_{\omega, \vec{k}}(\vec{r})$ for all lattice vectors \vec{R} . Restricting the Bloch vector to the first BZ, corresponds to a back-folding of the dispersion relation in the infinitely extended k-space into the first BZ by means of translations through reciprocal lattice vectors. This introduces a discrete band index $n \in N$ such that the band structure is described by the set $\{[\omega_n(\vec{k}), \vec{H}_{\omega, \vec{k}}^n], \vec{k} \in 1^{st} \text{ Brillouin zone}, n \in N\}$ of eigenfrequencies and eigenvectors associated with Eq. (1). To solve Eq. (1), we use the plane wave expansion method [9, 10]. In this method the Bloch component of the magnetic field is expanded in a set of transverse plane waves:

$$\vec{H}_{\omega, \vec{k}}(\vec{r}) = \sum_{\vec{G} \in 1^{st} \text{ BZ}} \sum_{\lambda=1,2} \vec{e}_{\lambda, \vec{k} + \vec{G}} u_{\vec{G}, \lambda}^{(\vec{k})} e^{i\vec{G} \cdot \vec{r}}, \quad (3)$$

where $\vec{e}_{\lambda, \vec{q}} \cdot \vec{q} = 0, \lambda = 1, 2$ are transverse unit vectors and $u_{\vec{G}, \lambda}^{(\vec{k})}$ are the expansion coefficients to be determined. Eq. (3) is then inserted into Eq. (1) through Eq. (2) leading to a standard hermitian eigenvalue problem [7]. For concreteness, we consider the case of a high refractive index ($n=3.45$) inverse opal. The corresponding band structure is shown in Fig. (1).

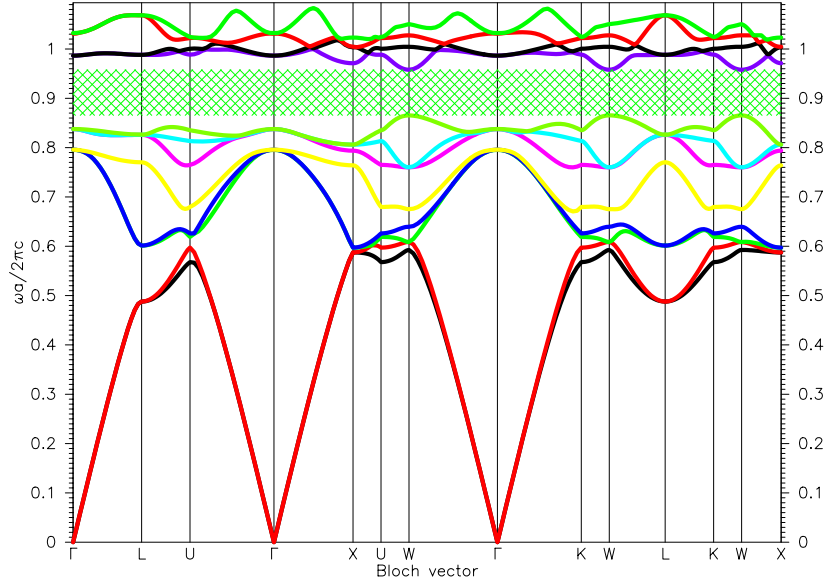


Fig. 1. Band structure for the inverse opal crystal with index 3.45. The radius of the air spheres is $0.364a$ and the solid dielectric coating thickness is $0.065a$ where a is the lattice constant of the fcc lattice. The \vec{k} vector runs along a few high symmetry directions in the fcc Brillouin zone. The full photonic band gap opens between normalized frequencies [0.87–0.96].

2 Optical field enhancement and trapping potential

The electric field for a mode of frequency ω may be calculated from Maxwell's equation:

$$\begin{aligned} \vec{E}(\vec{r}, t) &= \text{Re}(\vec{E}_{\omega}(\vec{r})e^{i\omega t}) \\ \vec{E}_{\omega}(\vec{r}) &= -\frac{ic}{\omega} \frac{\mathcal{N}}{\epsilon(\vec{r})} \vec{\nabla} \times \vec{H}_{\omega}(\vec{r}) \end{aligned} \quad (4)$$

where \vec{H}_ω is given by Eq. (2) and \mathcal{N} is a normalization constant. Fig. (2) shows frames from the movies that visualize the absolute value of the electric field, $|\vec{E}_\omega(\vec{r})|$, for the modes of band 8 and 9 at the W-point, corresponding to lower and upper band edge of the complete PBG of the silicon inverse opal. The movies show the absolute value of the electric field, $|\vec{E}_\omega(\vec{r})|$, on three orthogonal slices, $x = x_0, y = y_0, z = z_0$. In addition, the dielectric function is also represented by the warp applied to the orthogonal slices. The slices experience a small deformation in the solid component and no deformation in the air component. The frames in the movie correspond to different values for z_0 . Since the field is concentrated in the dielectric component or in voids, respectively, the modes are referred to as “dielectric mode” (band 8) and the “air mode”, respectively. In the dielectric mode, the peak optical intensity is 200 times that of a plane wave with the same average energy density. This redistribution and focusing of optical intensity may facilitate certain nonlinear optical effects in the solid.

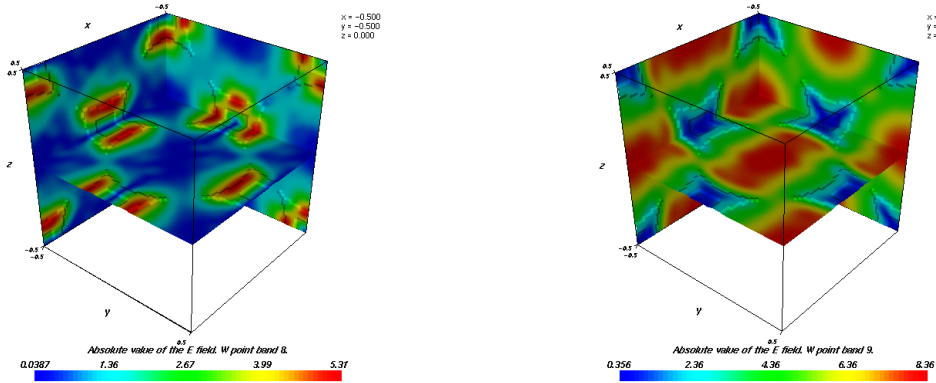


Fig. 2. The absolute value of the electric field in the modes corresponding to bands 8 and 9 at the W-point, respectively. $|\vec{E}_\omega(\vec{r})|$ is color-coded according to the color bar. The three orthogonal slices are warped by the value of the dielectric function with a zero displacement in the air component and a positive displacement in the Si component. The frames in the movies correspond to different values for the $z=\text{const}$ slice. The high-intensity regions of band 8 (1.3M) lie predominantly in the high dielectric region, thus representing a dielectric band while the high-intensity regions of band 9 (1.3M) are located within the air voids of the inverse opal, corresponding to an air band.

An atom placed in the field of the “air mode” will experience a force proportional to the gradient of the field’s optical intensity (proportional to the square of the modulus of the electric field). This so-called dipole force originates in the dynamical Stark-shift of the atom’s energy levels in the presence of the external field [11]. The energy shift of the atom’s ground state is proportional to the optical intensity of the field and its sign is determined by the detuning of the frequency of the external field from the atomic resonance. When the frequency of the external field is tuned below atomic resonance (red shifted) the atom will be attracted to the regions of high field intensity (“high-field seekers”) while for blue shifted fields the atom will be attracted to regions of low field intensity (“low-field seekers”). The dipole-force is derived from the potential [11]:

$$U(\vec{r}) = \frac{\hbar\delta}{2} \left(1 + \frac{I(\vec{r})}{I_{sat}} \frac{1}{1 + (2\delta/\gamma)^2} \right), \quad (5)$$

where δ is the detuning of the external field’s frequency from the atomic transition, $I_{sat} \equiv \pi\hbar c\gamma/3\lambda^3$ is the saturation intensity of the atomic transition and γ denotes the atom’s natural line width. Finally, $I(\vec{r})$ is the optical intensity of the field at the atomic position \vec{r} . As an example, we consider the 589.16 nm Na transition $3^2S_{1/2}-3^2P_{3/2}$ which

is characterized by a line width of $\gamma = 2\pi \times 10.01$ MHz and a saturation intensity of 6.40 mW/cm². Focussing a laser beam onto a small spot to achieve a peak intensity of $I/I_{sat} = 10^6$ and an optimal detuning of $2\delta/\gamma \approx 505$, the depth of the optical potential corresponds to about 100 mK. The peak intensity is 600 times greater than that of a plane wave with the same average energy density. This clearly demonstrates that optical trapping of cold atoms in photonic crystals may be achieved when the appropriate modes of the crystal are excited using a single external laser beam (“activating the trap”). Once the atomic transition has been selected, an inverse opal may be designed to trap atoms either in the high or low field regions depending on whether the detuning of the laser field from the atomic transition is negative or positive. Fig. (3) provides a different visualization of the optical intensity of the field. The movies display a sketch of the conventional fcc unit cell together with the iso-intensity surfaces $|\vec{E}_\omega(\vec{r})| = v$ of the dielectric and air mode, respectively, for different values v of the intensity. The optical trap for low and high-field seekers, respectively, is clearly visible.

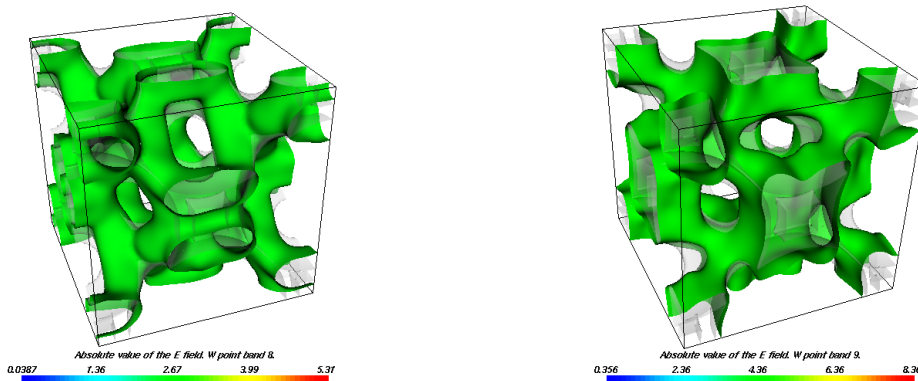


Fig. 3. The absolute value of the electric field in the modes corresponding to bands 8 and 9 at the W-point, respectively. $|\vec{E}_\omega(\vec{r})|$ is represented as a surface of constant value. The frames in the movies correspond to isosurfaces of different values and the color of the isosurface is mapped to the colorbar. The semi-transparent shape of the silicon backbone is also shown. Band 8 (2.1M) corresponds to the dielectric band, while band 9 (1.9M) represents an air band.

3 Optical cooling

Optical traps in general can store only relatively cold atoms. In addition to this limitation the red shifted traps with small detuning can cause a significant increase in the spontaneous emission and thus heat up the trapped atoms. It is, therefore, desirable to coordinate a cooling mechanism with the trapping action.

In contrast to optical trapping of a 2 level atom using the gradient of the field intensity, optical cooling below the Doppler limit utilizes polarization gradients on a multilevel atom. Cooling is based on the non-adiabatic response of moving atoms to the electromagnetic field which optically pumps the sub-levels of an atomic state (usually the ground state). An example is Sisyphus cooling in which the field is created by a pair of linear and cross-polarized counter-propagating plane waves. The resultant polarization cycles from linear to circular to orthogonal linear to opposite circular in a half wavelength [11].

In Fig. (4), we visualize the polarization gradients associated with the air mode discussed above, W-point band 9. The polarization state at an arbitrary position in space is described by the trajectory of the tip of the electric field. In general this is an ellipse which is characterized by its major axis \vec{M} , minor axis \vec{m} and a normal vector

$\vec{n} \equiv \vec{M} \times \vec{m}/|\vec{M}|^2$. When the tip of the \vec{E} field rotates from the major to the minor axis, the handedness of the polarization is given by the direction of the normal. The length of the normal varies from 0 for a linearly polarized state to 1 for a circularly polarized state. The ellipticity, Fig. (4) (left), is defined as the ratio between the lengths of the minor and major polarization axes. Very strong polarization gradients near the periphery of the optical traps are displayed in this mode. Fig. (4) (right) shows a frame from the movie which visualizes the major and minor polarization axes together with the normal to the polarization plane along a path in the photonic crystal. The polarization encountered along this path is very similar to the one expected in the lin \perp lin model of Sisyphus cooling [11].

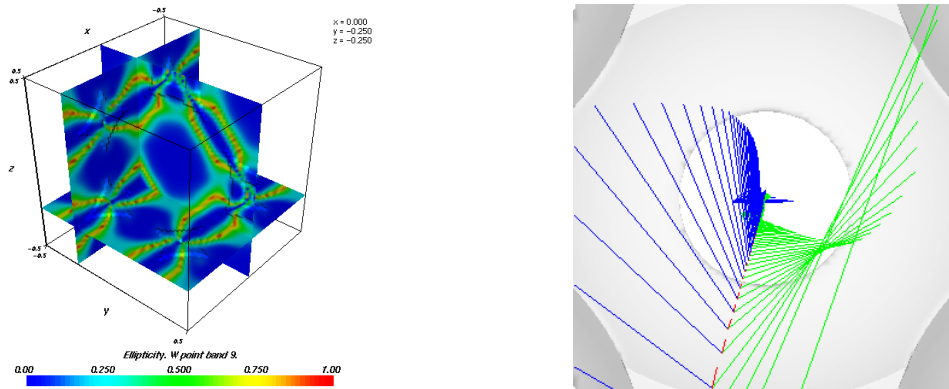


Fig. 4. [Left] The ellipticity in the air mode (band 9 at W-point) is color coded according to the color bar. A value of 0 corresponds to a linearly polarized state and a value of 1 corresponds to a circularly polarized state. The frames in the movie correspond to different values for the $x=\text{const}$ slice (1.4M). [Right] The major and minor polarization axes along a path passing entirely through the air component of the inverted opal in the same air mode. Major axis is colored blue, minor axis is green and the normal to the polarization plane is colored in red. The intersection of the path with the conventional unit cell runs from $\{x, y, z\} = \{0, -1/2, -1/2\}$ to $\{0, 1/2, 1/2\}$. (2.5M)

4 Discussion

In summary, we have shown that the dielectric and air bands at the lower and upper photonic band edge, respectively, provide a mode structure suitable for optical trapping of cold atoms. Low-field seekers may be trapped using the dielectric band and high-field seekers may be trapped using the air band. Also the blue-shifted optical field of a dielectric band will have an evanescent component in the void region. This can act as a repulsive optical potential to prevent the atom from colliding with the walls of the photonic crystal or for guiding matter waves through waveguide channels in the crystal. The trap may be activated by exciting the respective mode from a single laser, thus circumventing the need for complicated multi-laser setups of standard optical trapping technology. In addition, these modes exhibit sizeable polarization gradients which may facilitate optical cooling of atoms that are located in the photonic crystal. The combination of atom cooling and trapping effects with the control and suppression of spontaneous emission from the atoms may provide an avenue for the experimental observation of a number of novel quantum optical effects of cold atoms in a PBG material.

Acknowledgements

K.B. acknowledges the financial support of the Deutsche Forschungsgemeinschaft under Bu 1107/2-1 (Emmy-Noether programme).